



On Coherent Structures of Turbulent Open-channel Flow Above a Rough Bed

S. H. Mohajeri^a, S. Kazemi Mohsenabadi^b, M. Righetti^c

^aDepartment of Civil Engineering, Science and Research Branch, Islamic Azad University, Tehran, Iran.

^bDepartment of Civil Engineering, Buinzahra Branch, Islamic Azad University, Buinzahra, Iran.

^cFaculty of Science and technology, Free University of Bozen, Bozen, Italy.

PAPER INFO

Paper history:

Received 09 August 2016

Received in revised form 30 September 2016

Accepted 30 September 2016

Keywords:

Rough Bed

Turbulent Flow

Particle Image Velocimetry

Vortex Organization

Two-point Correlation

ABSTRACT

Present study examines turbulent structures of a rough bed open-channel flow in the context of deterministic approach. Instantaneous velocity field is measured in different hydraulic conditions using two dimensional Particle Image Velocimetry (PIV) in vertical plane and Stereoscopic PIV in horizontal plane. Different techniques and quantities such as swirl strength, two-point and cross-correlations of the swirl strength and fluctuating velocity are estimated to control formation of hairpin vortex. Our observations show in the area far above roughness elements, there is fairly a good agreement with the observations of previous studies for smooth-bed boundary flow. This consistency demonstrates that there is a similarity between outer region of the smooth and rough-bed layer flow. Moreover, some of the observations in the present study such as contourmap of instantaneous vorticity and swirling strength or observed inclination angle in contourmap of two-point correlations of the fluctuating velocity and swirl contourmap can be considered as signatures of the hairpin vortex. Given these observations, due to the lack of direct observation of the hairpin vortex and similarity of the observed features with signatures of other types of coherent structures, it is still too hard to assurly opine that in this condition, hairpin vortex is present.

doi: 10.5829/idosi.ije.2016.29.11b.05

NOMENCLATURE

D_{50}	Particle diameter at 50% passing	ρ_{zu}	Two-point correlations of velocity and swirling strength
D_{90}	Particle diameter at 90% passing	x_o, y_o	Reference point coordinate
Re	Reynolds Number	$\Delta x, \Delta y$	Spatial separation in the streamwise direction
Fr	Froude Number	σ_λ	Standard deviation of swirling strength
Δ^+	Dimensionless vertical roughness length scale	i, j, k	Indices refer to coordinate directions (1: streamwise, 2: spanwise, 3: vertical direction)
ν	Water Kinematic Viscosity	σ_u	Standard deviation of streamwise velocity
σ	Roughness representative length scale	U	Mean velocity
u_*	Shear velocity	ω	Spanwise vorticity
B/H	Aspect ratio	u_c	Convection velocity
B	Channel width	λ	Two-dimensional swirling strength
H	Water depth	ρ_u	Two-point correlations of velocity
S	Bed slope	u'	Instantaneous velocity fluctuation
X_L	Flow development length	v	spanwise velocity
u	Streamwise velocity	w	Vertical velocity

*Corresponding Author's Email: hossein.mohajeri@gmail.com (S. H. Mohajeri)

1. INTRODUCTION

Without any doubt, “*problem of turbulence*” which has been studied for more than 500 years, still is one of the most challenging issues. Turbulence is present in most fluid flows [1]. Moreover, because of the high diffusivity, turbulence drives significant mass and momentum transport [2]. Also, turbulence play a crucial role in many engineering processes such as combustion [3] or sediment and haze transport [4, 5]. Despite the high importance of turbulence, and its ubiquity, the problem of turbulence remains an unsolved problem to this day. For this reason, turbulence is still broadly investigated by the researchers and experts in various engineering disciplines such as mechanical engineers, geomorphologists, hydraulic engineers and environmental scientists.

To study turbulence, two different approaches are available [6]. The first one is a *statistical approach* which is based on the concept of energy cascade [2]. The prevalent tools in this approach are statistical methods including mean, standard deviation, skewness, flatness, spectra, cospectra and correlation analysis [7, 8]. More recently the study of coherent structures becomes popular as an approach that try to put order in the disorder of turbulence, detecting and depicting the main features of a turbulent flow field through the identification of the organized vortical structure –the so-called “*coherent structures*”–that mark the flow. Such coherent structures, which can be called eddies, can be interpreted as elementary organs of a turbulent flow [9]. In fact, by the definition, turbulent flow is composed of fluid whirls, which are the same as eddies, with various sizes. Great whirls gobble smaller whirls and feed on their velocity; but where great whirls grind, they also slow, and little whirls begin to grow - stretching out with high vorticity up to the limit of viscosity [10]. This approach promised an alternative to the frustrating verdict that turbulence can only be understood and tackled on statistical grounds. The approach in which turbulence is studied through the concept of coherent structures is known as *deterministic approach* [11-13]. Although statistical approach has been commonly used for a quite long time, recent development in measurements apparatus such as Particle Image Velocimetry (PIV), which provides spatial resolution instantaneous velocity in addition to time resolution, paves the ground for investigation of turbulent flow using deterministic approach [6].

One of the most common class of turbulent flow which has been studied by deterministic approach is boundary layer flow. Previous studies showed that in such flow, various coherent structures can be formed [9, 14]. The most famous coherent structures in boundary layer are upward movement of low-velocity flow and downward movement of high-velocity flow which are known as

sweep and ejection events [15, 16]. In early 2000s, following studies indicated that sweep and ejection events are part of a larger coherent structures which could be called *hairpin vortex* [11, 17]. In Figure 1, scheme of this vortex is shown [17]. As it can be seen, this vortex has two legs which lies on the bed and among these legs low velocity flow ejects upward. At the upper level, these two legs reach each other and form a head region. These elements together form a shape similar to the horseshoe or hairpin and due to this fact this structure is called hairpin vortex. As also shown in Figure 1, any increase in Reynolds number leads to a hairpin vortex which is more condensed and more stable [14]. It should be noted that, as convection velocity move the fluid in the streamwise direction, the ejection of the low-velocity is not fully orthogonal and it has generally an inclination [18].

As hairpin vortex is a three dimensional coherent structure [11] and till now, no cost-affordable instrument has not been developed to resolve 3D instantaneous flow field, direct observation of such a structure is not straightforward. This measurement limitation causes that hairpin vortex is generally detected by some of its effects and impingings [9]. These impingings, which are known as *hairpin vortex signatures* [9, 18, 19] are shown in Figure 2. As shown, hairpin vortex signatures are consisted of the ejection flow with an orientation approximately perpendicular to the plane containing the head and the neck of the hairpin and the low-speed streak next to the bed. Also, there will be an area with high vortex in the border of these two areas.

Although there is enough evidence that hairpin vortex is present in turbulent smooth bed boundary layer flow [11, 14, 18], presence of such structure in rough bed boundaries is questionable [20, 21]. In some of turbulent rough bed studies, the presence of hairpin vortex has been observed [22], but some other studies could not depict the hairpin vortex signatures [23]. Instead, other types of coherent structures such as funnel-shaped Vortex has been suggested for such flow [23, 24].

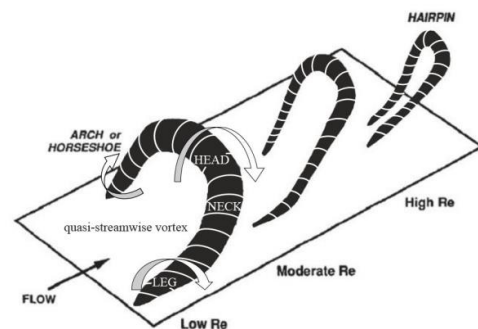


Figure 1. Schematic view of hairpin vortex, modified from Dennis [14].

This study focuses on the examination of turbulent rough bed boundary layer flow through deterministic approach. Specifically, the presence of hairpin vortex signatures in such environment will be controlled using experimental data measured by Particle Image Velocimetry (PIV). To this end, two series of PIV data in horizontal and vertical planes are measured in an open channel with a bed roughened using gravel particles. These experiments will be described in the following section.

2. EXPERIMENTAL APPARATUS

The experiments were conducted in a 0.4 m wide, 0.4 m deep, and 6 m long rectangular tilting open channel at the Hydraulic Engineering Laboratory of the University of Trento. The flume bed was covered by a layer of gravel 20 cm thick. The flow depth was controlled by an adjustable tailgate installed at the end of the flume. The discharge at the flume inlet was controlled by an inverter for pump speed regulation, and was measured by an electromagnetic flowmeter. In Figure 4-a, schematic view of open-channel is shown. In our study, we employ the right-hand coordinate system, i.e., the x -coordinate is oriented along the main flow positive downstream and parallel to the mean bed, with its origin $x=0$ located 3.3 m from the flume inlet; the z -coordinate refers to the vertical direction, pointing upward from the gravel tops; and the spanwise y -axis is directed to the left wall.

Gravel material with $D_{50}=22$ mm and $D_{90}=29$ mm (D_{50} and D_{90} are the particle diameters at 50% and 90% passing) was spread uniformly on the channel bottom to create a homogeneous gravel-bed layer (Figure 3). The bed topography was measured by a M5L/200 laser scanner covering a bed region above which velocity measurements were made.

Three experimental scenarios (named Run I, Run II and Run III) were studied, covering a range of hydraulic conditions with different values of Reynolds number;

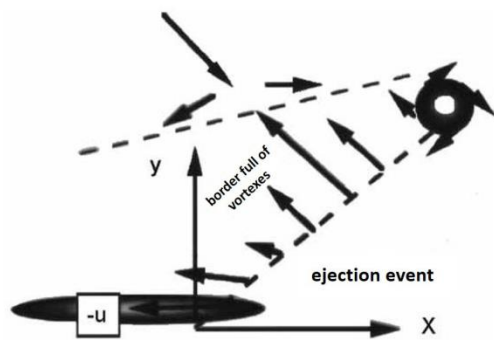


Figure 2. Hairpin vortex signatures, modified from Adrian et al. [17].

while maintaining the Froude number almost constant (see Table 1). In Table 1, dimensionless vertical roughness length scale $\Delta^+ = u_* \sigma / \nu$ (where u_* is shear velocity, ν is kinematic viscosity and σ is equal to the standard deviation of local bed elevations as suggested by Nikora et al. [25] which is $\sigma = 6.1$ mm in present study) are much higher than 5 which is the rough estimate of dimensionless viscous sublayer thickness [26]. This means that the studied flows exhibited a hydraulically-rough bed condition. In all cases, the aspect ratio was higher than five suggesting that effects of secondary currents in the central part of the flow should not be significant [27]. Table 1 also shows u_* obtained by extrapolation of the double averaged Reynolds shear stress profile to the gravel crest as proposed by Pokrajac et al. [28].

Free surface profiles along the whole flume length were measured by an ultrasonic distance transducer with 20 cm sampling interval, along the channel centerline. Uniform flow conditions were checked by comparing water surface slope to bed slope which ranged within 0.0026-0.0029 (Table 1). Flow development lengths for the three runs were estimated as in Nikora, Goring and Biggs [29] using a concept of the internal boundary layer of Monin and Yaglom [7] and are reported in Table 1.



Figure 3. Bed roughness in present experiments.

TABLE 1. Hydraulic Conditions of Experimental Runs

	Run I	Run II	Run III
H (m)	0.040	0.052	0.060
S (-)	0.0028	0.0026	0.0029
Fr (-)	0.51	0.47	0.51
Δ^+ (-)	170	201	250
$Re \times 103$ (-)	12.75	17.63	23.32
B/H (-)	10.0	7.7	6.7
Q (10-3 m ³ /s)	5.1	7.05	9.33
XL (m)	1.37	1.61	1.74
u^* (m/s)	0.028	0.033	0.041

Measurements were performed in a flow region at least 150 mm far from both side walls at the distance of 3.3 m from the entrance of the channel, where the velocity profile is fully developed while effects of the downstream weir remain negligible.

Two series of time-resolved PIV measurements in vertical and horizontal planes, as shown in Figure 4-b, were carried out. In the first series of measurements, stereo PIV was applied to measure three velocity components (u , v and w) in the x - y (horizontal) plane located 1 mm above the crests (i.e., 2-dimensional 3-component PIV, 2d3c). The acquisition area was approximately 140 mm long and 140 mm wide, with its center placed approximately at the middle of the channel.

In the second series of measurements, 2-dimensional 2-component (2d2c) PIV was used to measure flow fields at three vertical x - z -planes located at the centerline, 50 mm left, and 50 mm right of the channel center, as shown in Figure 4-b. In Figure 4-b, planes 1, 2 and 3 refer to 2d2c measurement planes. In all measurements, high-speed Fastcam X 1024 PCI Photron cameras with a super light sensitive 10-bit CMOS sensor were used. The laser was a Nd:Yag in continuous mode. Sieved pollen particles were used as seeding material. For each run, the seeding material was injected at the entrance of the channel. To eliminate the domains occupied by the bed in the images, a mask based on the measured bed elevations was prepared and applied to the data. The measurement regions were $1024 \times 512 \text{ px}^2 \approx 128 \times 64 \text{ mm}^2$ in the vertical planes and $1024 \times 1024 \text{ px}^2 \approx 140 \times 140 \text{ mm}^2$ in the horizontal plane. For each run, in total, three vertical planes covered at least 12 large bed gravel particles along the x -direction.

The image analysis and processing were performed with PIVDEF software (CNR-INSEAN) [30]. The resulted vector spacing was approximately 1 mm in both horizontal and vertical planes. For each experiment, the sampling frequency was 500 Hz. Flow was sampled for 38.4 s in vertical-plane measurements and for 13 s in horizontal-plane measurements. Cooper and Tait [31] specifically studied the effects of PIV measurement setup on velocity statistics over gravel beds. Comparison of our measurement duration with Cooper and Tait [31] measurement duration shows that the measurement in the vertical planes were long enough to ensure statistical convergence for at least low-order moments of the flow field. Although the measurement duration in the horizontal plane seems fairly short for obtaining the reliable statistics, it appears sufficient for our analyses as its spatial equivalent exceeds 60 flow depths (Taylor's frozen turbulence hypothesis was used here for converting time domain into spatial domain). More information about PIV setup and also measurements errors can be found in Mohajeri, Grizzi, Righetti, Romano and Nikora [32].

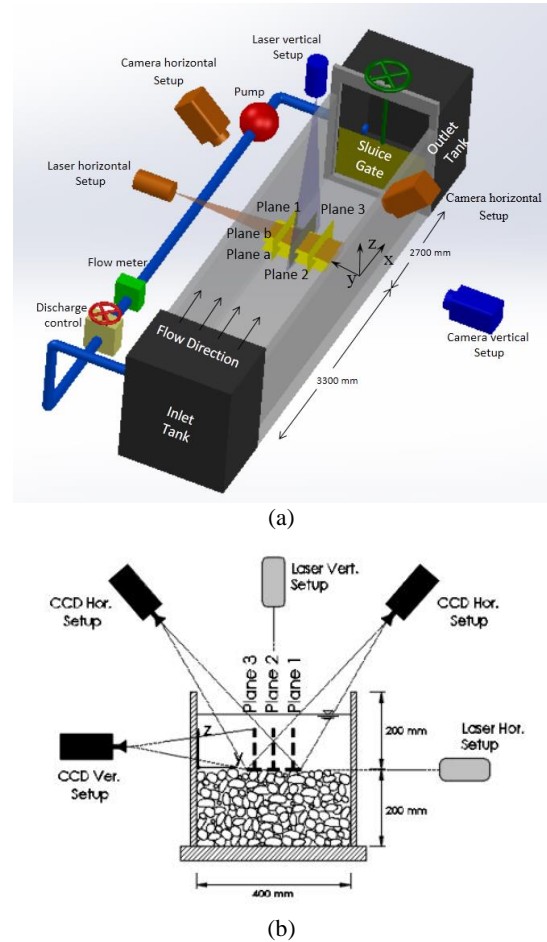


Figure 4. a) Schematic view of open-channel b) Streamwise view showing both conventional 2-component and stereoscopic 3-component PIV set-ups

3. RESULTS

3. 1. Instantaneous Vortical Structure

To investigate instantaneous flow structure, in Figure 5a,b two snapshots sequence of instantaneous vorticity field accompanying with vector field measured in vertical plane 3 for Run (I) is shown. The time lag between these two snapshots is so small (80 millisecond) which assure that Figure 5a,b describe a similar event, but at different times. The background color maps in Figure 5 a,b refer to spanwise vorticity which can be determined as:

$$\omega_k = \frac{1}{2} \left(\frac{\partial u_j}{\partial x_i} - \frac{\partial u_i}{\partial x_j} \right) \quad (1)$$

Note that the indices in Equation (1) for spanwise vorticity are ω_k and $i=1, j=2$. The velocity vector field in Figure 5 is decomposed based on the Galilean approach with convective velocity $u_c=[0.85U, 0]$ instead of Reynolds decomposition [33].

The main reason for this choice is that the shear between structures with Galilean decomposition is preserved. Also, as Navier-Stokes equations are not sensitive to Galilean transformation, the convection velocity can be considered directly in the Navier-Stokes equations with no necessity to Reynolds stress modification [17]. It is worthy to note that the value of convection velocity in Figure 5 obtained from a try and error process for better visualization of instantaneous vector field.

In the boundary layer flows, the background shear is significant and vorticity solely cannot identify vortices properly [12, 34]. In order to solve this problem, complex Eigen values of velocity gradient tensor have been widely used [11, 12]. λ defined as in Equation (3) is used to identify vortex cores:

$$\lambda_k = \max\left[0, -\frac{\partial u_i}{\partial x_j} \frac{\partial u_j}{\partial x_i} + \frac{1}{2} \frac{\partial u_i}{\partial x_i} \frac{\partial u_j}{\partial x_j} - \frac{1}{4} \left(\frac{\partial u_i}{\partial x_i}\right)^2 - \frac{1}{4} \left(\frac{\partial u_j}{\partial x_j}\right)^2\right] \quad (2)$$

Lines of constant value of spanwise swirling strength (λ_3 and $i=1, j=2$) are shown in Figure 5c,d with red color. Moreover, the color maps in Figure 5 c,d refers to fluctuating part of streamwise velocity. In both of snapshots, there is a good agreement between information obtained from vorticity, velocity and swirling strength fields. In Figure 5a, wedge-like structure of the flow field is recognizable, with two well noticeable regions of high velocity and low velocity. Similar features of the flow field were present also in all the vertical planes of other runs. The shear layer between these regions is inclined in streamwise

direction. Contour lines of swirling strength show that the strip at the inclined shear layer, located just at the boundary of high and low velocity regions, is rich of small eddies. These eddies typically initiates at gravel crests and move downstream with positive normal velocity, so transferring to upper part of the flow field. Vortices are stronger near the bed and attenuate during their flapping transport and stretching moving downstream. However, in many instants it has been observed that these packets are able to reach the water surface. These features are consistent with previous findings of Roy and et al. [23] and Detert, Nikora and Jirka [20].

In Figure 6, similar to Figure 5, two sequence snapshots of instantaneous vorticity, Galilean decomposed vector field ($u_c=[0.53U, 0]$), swirling strength, and streamwise velocity fluctuation are shown for the horizontal layer acquisition in Run (I). In Figure 6, vortices are generated and then transported downstream. Meanwhile they convey downstream, they get out of the measurement layer.

Also, typical picture of streaky structure of elongated high and low velocities can be identified. Similar streaky structure has been observed in previous studies above rough bed [20, 35, 36]. Specifically, previous studies observed longitudinal elongation of positive and negative vortices which is quite similar to what can be depicted in Figure 6.

While streaky structure in rough beds was seen in Figure 6, it is worth to be noted that in some regions there are also persistency of vertical axis vortex presence. As an example, some regions are highlighted with yellow circle dashed lines, which are the regions of strong protrusion of isolated gravel crest.

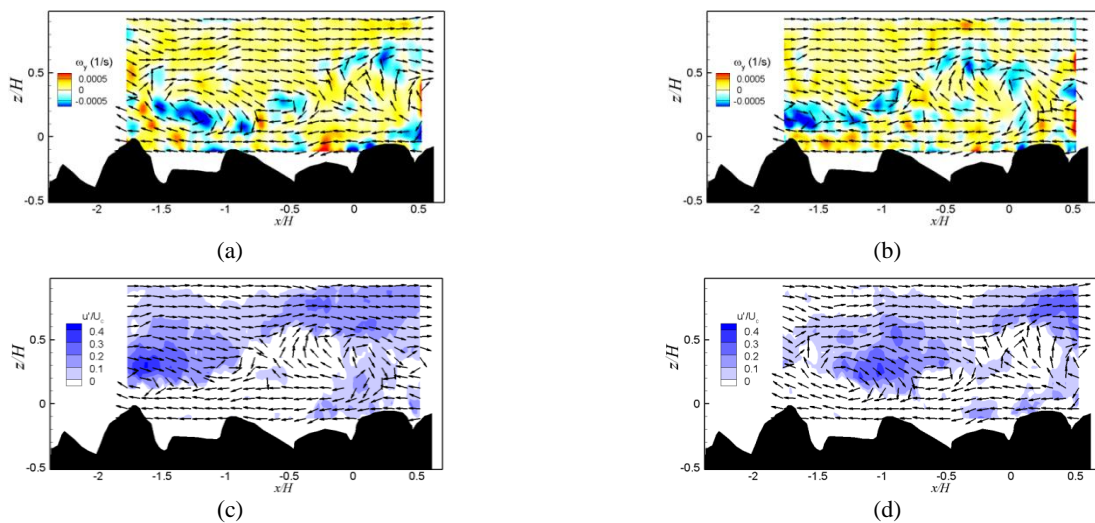


Figure 5. Sequence of two snapshots of instantaneous velocity fields in Run (I), vertical plane 3, in a) and b) colour map shows vorticity and vector based on Galilean decomposition, while in c) and d) colour map shows streamwise velocity fluctuation and red lines swirling strength. Flow from left to right

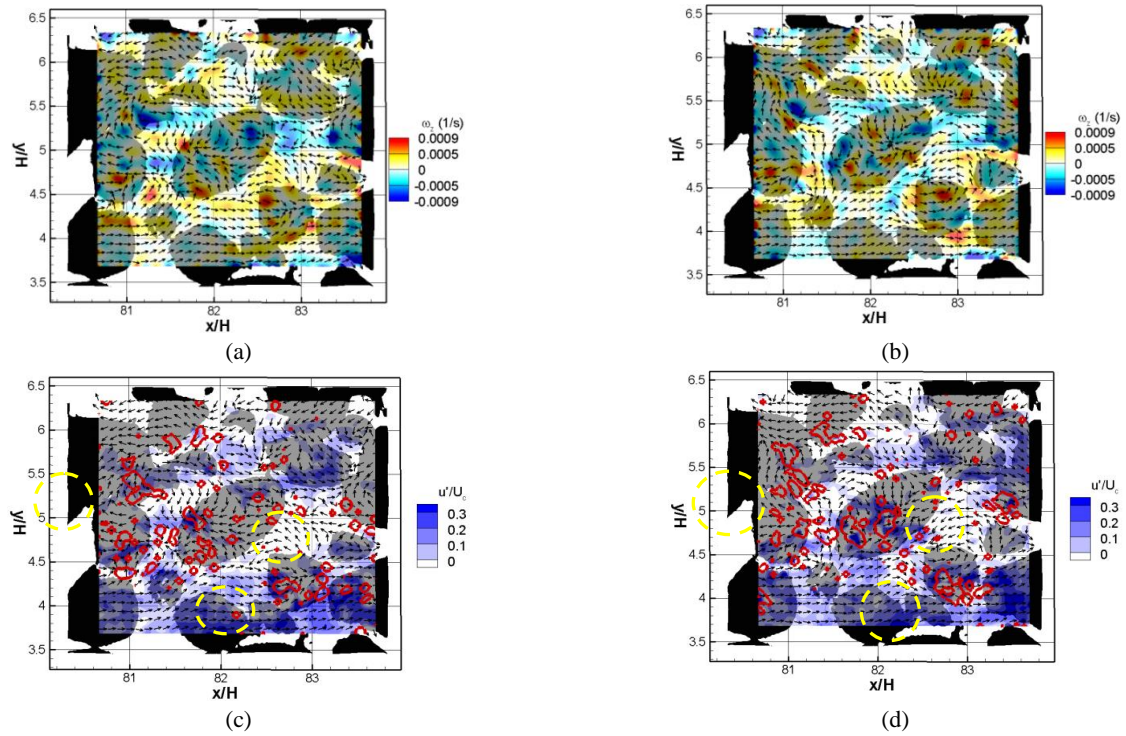


Figure 6. Sequence of two snapshots of instantaneous velocity fields in Run (I) and at gravel crest, In (a) and (b) plots colour map shows vorticity and vector based on Galilean decomposition, In (c) and (d) plots colour map shows streamwise velocity fluctuation and red lines swirling strength.

In these regions, vortices generate and then convey downstream through streaky structure. This shows that unlike smooth walls, locations of vortices generation do not distribute randomly through bottom of the channel and they are mostly occurred around gravel crests.

3. 2. Correlation Functions To further explore presence of coherent structures, the statistical characteristics of flow should be considered. In this regard, the two-point correlation between velocity components can show further properties of coherent structures [18, 21]. Specifically, the two-point correlations of streamwise velocity are utilized to explore the impact of bed roughness elements on the average extent and shape of the coherent structures. The correlations in both horizontal and vertical planes are computed as [33]:

$$\rho_u = \frac{\overline{u'(x_o, y_o)u'(x_o + \Delta x, z_o + \Delta z)}}{\sigma_u^2} \quad (3)$$

where, overbar denotes averaging across the ensemble values. In Figure 7, the contourmap of ρ_u in plane 2 for Run II is shown. In this figure, the reference point is $(x_o=0, z_o=13 \text{ mm})$. Note that the vertical location of reference point is selected so that it would be comparable to the size of roughness elements. Contourmaps in Figure 2 display the streamwise-

elongated coherence and slight inclination away from the bed. The slight inclination in the contour map of ρ_u is in agreement with slight inclination in hairpin vortex signatures shown in Figure 2. The overall shape of the contour map in Figure 2 is consistent with the hairpin vortex packets often observed in the outer-layer of smooth-bed turbulence [17, 18]. However, more precise comparison between Figure 2 and reported observations of hairpin vortex in smooth beds shows that a substantial reduction in the streamwise coherence of ρ_u is noticeable. Similar reduction of ρ_u is also observed by previous researchers [21, 22]. Guala et al. [21] represented that this reduction is mostly caused by a superposition of existing large-scale motions in the outer layer and small-scale structures shed from the roughness elements at the bottom of the channel. Although the spacing between roughness elements in Guala et al. [21] is much higher than the spacing between gravel particles of this study, their reasoning can be still valid and it is mostly probable that vortex shedding around gravel crests attenuated the streamwise velocity correlation.

The signatures of coherent structures from the vertical measurement planes are consistent with flow features revealed from the horizontal measurement planes which are discussed below. The results of ρ_u in horizontal plane and Run II is shown in Figure 8.

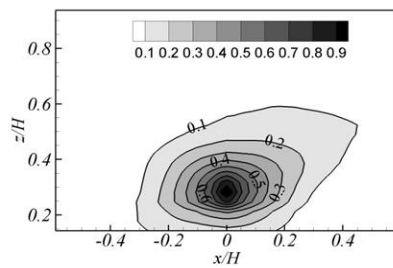


Figure 7. Contourmaps of ρ_u in plane 2, Run II

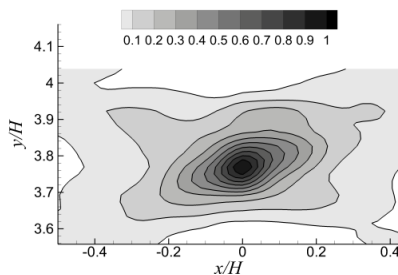


Figure 8. Contourmaps of ρ_u in horizontal plane, Run II

The figure shows that the long positive streamwise correlations of ρ_u are present. These features can be resulted by the presence of long low-speed regions such as those noted to occur within vortex packets. The same observations are also reported in previous studies. In the case of smooth bed, Ganapathisubramani et al. [18] observations reveals such longitudinal positive correlation due to the presence of hairpin vortex packets legs. Volino et al. [22] observations are conformal to what observed in present study. Moreover, they also observed secondary correlation peaks of both positive and negative values which are not detectable in Figure 8. This difference arises from the difference in the measurement configuration of present study and Volino et al. [22] study. Measurements in present study are done in an open channel, while Volino et al.'s [22] measurements are conducted in a wind tunnel.

Lateral spacing between velocity streaks is scaled with water depth in open channel and length of boundary layer in wind tunnel. As the size of PIV measurement in present study is almost the same as Volino et al. [22], due to the difference in lateral spacing of velocity streaks in open channel and wind tunnel, in present study the number of the revealed streaks is lower than Volino et al.'s [22] study and we cannot see the secondary correlation peaks. The contourmaps of Volino et al. [22] for smooth and rough bed measurements show that presence of bed roughness can reduce streamwise elongation of positive correlations. Despite the fact that in present study, only flow with rough bed are measured, our contourmap in Figure 8 are

mostly consistent with Volino et al. [22] ρ_u contourmaps for rough bed condition.

For better highlighting the specific features of hairpin vortex packet, conditional statistics must be considered. To this end, the two-point correlation functions between swirling strength and velocity is necessary as an objective measure of the conditionally averaged velocity field associated with the vortex heads [20, 37]. This parameter which is shown by $\rho_{\lambda u}$ can be defined as:

$$\rho_{\lambda u} = \frac{\overline{\lambda(x_o, y_o) u'(x_o + \Delta x, z_o + \Delta z)}}{\sigma_u \sigma_\lambda} \quad (4)$$

In Figure 9, contourmap of $\rho_{\lambda u}$ for Run II and in Plane 2 is shown. The reference point in this figure is $(x_o=0, z_o=26 \text{ mm})$. The vertical position of the reference point is changed for better visualization of hairpin vortex in the outer layer. The streamwise correlation functions are strongest near the reference line point. Moreover, $\rho_{\lambda u}$ is negative below and positive above z_o . This behavior is entirely consistent with the correlation between a region of strong swirling strength and the velocity vector pattern of a hairpin vortex head which, by definition, has a clockwise rotation. A key feature of this contourmap is a narrow large-scale interface region separating domains of positive and negative values of $\rho_{\lambda u}$. Such interface has mild inclination with inclination angle approximately similar to those observed for ρ_u in Figure 7. These findings suggest that the instantaneous structures occur with sufficient frequency, strength and order to leave an impinging on the flow statistics.

In the case of smooth bed turbulent flow, similar observations, but much clearer is also reported by Christensen and Adrian [37]. They suggest that such characteristics are statistical evidence of hairpin vortex packets in bed turbulence. For rough bed flows, the contourmap of $\rho_{\lambda u}$ in Detert et al. [20]'s study is also similar to what has been described in present study. Although they confirm it could be possible that these features are consistent with hairpin vortex packet signatures, they pointed out that relative submergence can affect such observation.

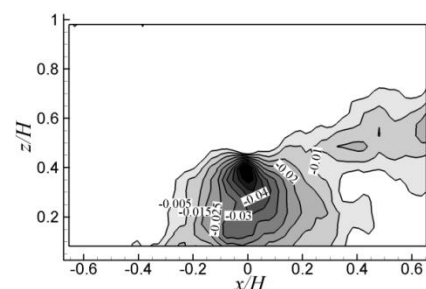


Figure 9. Contourmaps of $\rho_{\lambda u}$ in plane 2, Run II

4. CONCLUSIONS AND DISCUSSION

Present study deals with the coherent structures of boundary layer turbulent flow in an open channel with rough bed. Specifically, the main aim of this study is to explore the presence of hairpin vortex in rough bed turbulent flow. Despite presence of enough evidence that hairpin vortex packet is formed in smooth-bed turbulent flow, protrusion of bed roughness elements and vortex shedding in roughness layer can affect the outer layer and consequently formation of coherent structures in the area far from the bed.

Instantaneous velocity fields in present study mark that some coherent structures are still present in the rough bed boundary layer flow. Visualization of instantaneous velocity in vertical planes (Figure 5) shows that two fluid regions of fast and slow regions representing which respectively interpreted as an region with dominance of sweep and ejection events occurrence are present. There is also an interface border between these two regions which is full of vortexes. These vortexes convey simulatanoulsy in upward and streamwise directions. Moreover, horizontal plane observations (Figure 6) declare formation of low and high speed velocity streaks which can be interpreted as the legs of hairpin vortex packets. In overall, these observations are in agreement with hairpin vortex signitures which are shown in Figure 2.

Conformal to the observations in the instantaneous velocity characteristics, time-averaged characteristics also represents other evidence for presence of hairpin vortex packets. The results of two-points correlations in vertical and horizontal planes (Figures 7 and 8) are in agreement with the observations of the same parameters in smooth-bed turbulent flow. However, some slight differences are also notified. The streamwise elongation of contourmaps are shrinked in the case of rough-bed measurement in the present study. Previous studies of rough bed turbulent flow also reported similar behavior (e.g. [21, 22]) and they explain that this reduction can be the results of near bed roughness elements vortex shedding.

To further control the formation of hairpin vortex in such condition, two-point correlation of swirling strength and velocity fluctuation is estimated. The features of this figure is also conformal to the previous observations for the condition that hairpin vortex is present.

Although most of the described observations are consistent with hairpin vortex packets formation and probably hairpin vortex can form in such condition, one should noted that the authors can not confidently claim that the hairpin vortex is present. In fact, as explained in the introduction, it is not possible to directly see the hairpin vortex packets and we only use some signatures to control the presence of this structure. In other words, it is likely that other types of coherent structures, which

has some signatures similar to hairpin vortex, is formed. For example, some features of funnel shape vortex features proposed by Kaftori et al. [38] are consistent with hairpin vortex packet and as Roy et al. [23] believe this structure can be formed in open channel flow with rough bed. To assure that hairpin vortex is present in this condition, one should use quite expensive and advanced techniques such as holographic PIV to capture three components of velocity in the three dimensional domain. Therefore, it can be concluded that although most of the observations in present study demonstrate formation of the hairpin vortex, it is not possible to certainly claim that this features are belong to a hairpin vortex.

Finally, it should be highlighted that the observations in present study are some clues for presence of hairpin vortex in the outer region. Using such observation, it is difficult to deny lack of presence of other types of coherent structures, especially in the near bed region. Particularly, an assumption could be simultaneous presence of different types of coherent structures. In this regards, Bomminayuni and Stoesser [39] show that different types of turbulent structures are present around roughness elements. The concurrent presence of these different structures can cause formation of different turbulent structures (composed of coherent or instantaneous structures) in the outer layer which means that the effects and signatures of hairpin vortex (or other types of coherent structures) can be superposed. Future studies should be examine the accuracy of such an assumption.

6. REFERENCES

1. Pope, S.B., "Turbulent flows." (2001), IOP Publishing.
2. Tennekes, H. and Lumley, J.L., "A first course in turbulence, Pe Men Book Company, (1972).
3. Peters, N., "Turbulent combustion, Cambridge University Press, (2000).
4. Fernando, H.J., "Handbook of environmental fluid dynamics, volume two: Systems, pollution, modeling, and measurements, Taylor & Francis, (2012).
5. Mohajeri, S.H., Righetti, M., Wharton, G. and Romano, G.P., "On the structure of turbulent gravel bed flow: Implications for sediment transport", *Advances in Water Resources*, Vol. 92, , (2016), 90-104.
6. Nezu, I. and Nakagawa, H., "Turbulence in open channel flows, Taylor & Francis, (1993).
7. Monin, A. and Yaglom, A., "Statistical fluid mechanics - vol 1: Mechanics of turbulence, The MIT Press, (1971).
8. Javid, S. and Mohammadi, M., "Boundary shear stress in a trapezoidal channel", *IJE Transactions A: Basics*, Vol. 25, No. 4, (2012), 323-332.
9. Adrian, R.J., "Hairpin vortex organization in wall turbulence", *Physics of Fluids*, Vol. 19, No. 4, (2007), 413-420.
10. Hunt, J.C.R., Eames, I., Westerweel, J., Davidson, P.A., Voropayev, S., Fernando, J. and Braza, M., "Thin shear layers – the key to turbulence structure?", *Journal of Hydro-Environment Research*, Vol. 4, No. 2, (2010), 75-82.

11. Adrian, R.J., Christensen, K.T. and Liu, Z.C., "Analysis and interpretation of instantaneous turbulent velocity fields", *Experiments in Fluids*, Vol. 29, No. 3, (2000), 275-290.
12. Jeong, J. and Hussain, F., "On the identification of a vortex", *Journal of Fluid Mechanics*, Vol. 285, (1995), 69-94.
13. Nourollahi, M., Farhadi, M. and Sedighi, k., "Modified structure function model based on coherent structures", *IJE Transactions B: Applications*, Vol. 26, No. 5, (2013), 523-532.
14. Dennis, D., "Coherent structures in wall-bounded turbulence", *An. Acad. Bras. Cienc.*, Vol. 87, No. 2, (2015), 1161-1193.
15. Lu, S.S. and Willmarth, W.W., "Measurements of the structure of the reynolds stress in a turbulent boundary layer", *Journal of Fluid Mechanics*, Vol. 60, No. 03, (1973), 481-511.
16. Grass, A.J., "Structural features of turbulent flow over smooth and rough boundaries", *Journal of Fluid Mechanics*, Vol. 50, No. 02, (1971), 233-255.
17. Adrian, R.J., Meinhart, C.D. and Tomkins, C.D., "Vortex organization in the outer region of the turbulent boundary layer", *Journal of Fluid Mechanics*, Vol. 422, No., (2000), 1-54.
18. Ganapathisubramani, B., Hutchins, N., Hambleton, W., Longmire, E. and Marusic, I., "Investigation of large-scale coherence in a turbulent boundary layer using two-point correlations", *Journal of Fluid Mechanics*, Vol. 524, (2005), 57-80.
19. Marusic, I., McKeon, B., Monkewitz, P., Nagib, H., Smits, A. and Sreenivasan, K., "Wall-bounded turbulent flows at high reynolds numbers: Recent advances and key issues", *Physics of Fluids*, Vol. 22, No. 6, (2010), 651-660.
20. Detert, M., Nikora, V. and Jirka, G.H., "Synoptic velocity and pressure fields at the water-sediment interface of streambeds", *Journal of Fluid Mechanics*, Vol. 660, (2010), 55-86.
21. Guala, M., Tomkins, C.D., Christensen, K.T. and Adrian, R.J., "Vortex organization in a turbulent boundary layer overlying sparse roughness elements", *Journal of Hydraulic Research*, Vol. 50, No. 5, (2012), 465-481.
22. Volino, R.J., Schultz, M.P. and Flack, K.A., "Turbulence structure in rough- and smooth-wall boundary layers", *Journal of Fluid Mechanics*, Vol. 592, (2007), 263-293.
23. Roy, A., Buffin-Bélanger, T., Lamarre, H. and Kirkbride, A.D., "Size, shape and dynamics of large-scale turbulent flow structures in a gravel-bed river", *Journal of Fluid Mechanics*, Vol. 500, (2004), 1-27.
24. WeHsi, J.C., Yamane, Y., Yamamoto, Y., Egashiral, S. and Nakagawa, H., "Dye visualization and piv analysis of streamwise vorticity structure in a smooth-bed open channel flow", *Proceedings of Hydraulic Engineering*, Vol. 44, (2000), 491-496.
25. Nikora, V., Goring, D. and Biggs, B., "On gravel-bed roughness characterization", *Water Resources Research*, Vol. 34, No. 3, (1998), 517-527.
26. Mayes, C., Schlichting, H., Krause, E., Oertel, H.J. and Gersten, K., "Boundary-layer theory, Springer Berlin Heidelberg, (2003).
27. Nezu, I. and Nakagawa, H., "Turbulence in open-channel flows, A.A. Balkema, (1993).
28. Pokrajac, D., Finnigan, J.J., Manes, C., McEwan, I. and Nikora, V., "On the definition of the shear velocity in rough bed open channel flows", in *River Flow*, Lisbon, Portugal, Taylor & Francis. (2006).
29. Nikora, V., Goring, D. and Biggs, B., "Silverstream eco-hydraulics flume : Hydraulic design and tests", *New Zealand Journal of Marine and Freshwater Research*, Vol. 32, (1998), 607-620.
30. Di Florio, D., Di Felice, F. and Romano, G.P., "Windowing, re-shaping and re-orientation interrogation windows in particle image velocimetry for the investigation of shear flows", *Measurement Science and Technology*, Vol. 13, No. 7, (2002), 953-962.
31. Cooper, J. and Tait, S., "Spatially representative velocity measurement over water-worked gravel beds", *Water Resources Research*, Vol. 46, No. 11, (2010), W11559.
32. Mohajeri, S.H., Grizzi, S., Righetti, M., Romano, G.P. and Nikora, V., "The structure of gravel-bed flow with intermediate submergence: A laboratory study", *Water Resources Research*, Vol. 51, No. 11, (2015), 9232-9255.
33. Pope, S.B., "Turbulent flows, New York, Cambridge University Press, (2000).
34. Hunt, J.C.R., Wray, A.A. and Moin, P., "Eddies, stream, and convergence zones in turbulent flows", *Center For Turbulence Research*, Vol. Report CTR-S88, (1988).
35. DeFina, A., Transverse spacing of low-speed streaks in a channel flow over a rough bed, in *Coherent flow structures in open channels*, S.L.B. P. J. Ashworth, J. L. Best, S. J. Mc Lelland, Editor. (1996).
36. Nino, Y. and Garcia, M.H., "Experiments on particle—turbulence interactions in the near-wall region of an open channel flow: Implications for sediment transport", *Journal of Fluid Mechanics*, Vol. 326, (1996), 285-319.
37. Christensen, K.T. and Adrian, R.J., "Statistical evidence of hairpin vortex packets in wall turbulence", *Journal of Fluid Mechanics*, Vol. 431, (2001), 433-443.
38. Kaftori, D., Hetsroni, G. and Banerjee, S., "Funnel-shaped vortical structures in wall turbulence", *Physics of Fluids*, Vol. 6, No. 9, (1994), 3035-3050.
39. Bomminayuni, S. and Stoesser, T., "Turbulence statistics in an open-channel flow over a rough bed", *Journal of Hydraulic Engineering*, Vol. 137, No. 11, (2011), 1347-1358.

On Coherent Structures of Turbulent Open-channel Flow Above a Rough Bed

S. H. Mohajeri^a, S. Kazemi Mohsenabadi^b, M. Righetti^c

^a Department of Civil Engineering, Science and Research Branch, Islamic Azad University, Tehran, Iran.

^b Department of Civil Engineering, Buinzahra Branch, Islamic Azad University, Buinzahra, Iran.

^c Faculty of Science and technology, Free University of Bozen, Bozen, Italy.

PAPER INFO

چکیده

Paper history:

Received 09 August 2016

Received in revised form 30 September 2016

Accepted 30 September 2016

Keywords:

Rough Bed

Turbulent Flow

Particle Image Velocimetry

Vortex Organization

Two-point Correlation

مطالعه حاضر به بررسی جریان در یک کانال روباز با بستر زیر براساس رویکرد قطعی در مطالعه جریان آشفته می‌پردازد. به این منظور، سرعت لحظه‌ای جریان توسط روش سرعت‌سنجی تصویری به کمک ذرات اندازه‌گیری شد. بردارهای لحظه‌ای سرعت در این شرایط در دو سری برداشت در صفحات قائم و افقی اندازه‌گیری گردیدند. از کمیت‌ها و روش‌های مختلفی مانند قدرت پیچش، همبستگی دونقطه یا خود همبستگی سرعت نوسانی و قدرت پیچش که در رویکرد قطعی مطالعه جریان آشفته رایج می‌باشند، برای کنترل تشکیل یا عدم تشکیل گردابه به شکل سنجاق موی سر بهره برده شد. مشاهده شد که در نواحی دور از بستر زیر، تطابق قابل قبولی بین مشاهدات مطالعه حاضر و مشاهدات مطالعات پیشین در جریان آشفته با بستر صاف وجود دارد. این تطابق نشان می‌دهد که لایه خارجی جریان آشفته در بستر زیر و بستر صاف دارای تشابه مناسبی با یکدیگر هستند. بررسی‌های بیشتر نشان داد که بسیاری از مشاهدات مطالعه حاضر، مانند نحوه تغییرات خطوط تراز منحنی‌های قدرت پیچش و ورتیسته جریان و یا زاویه انحراف در خطوط تراز منحنی‌های همبستگی دونقطه‌ای سرعت، با ویژگی‌های گردابه به شکل سنجاق موی سر در تطابق می‌باشد. با وجود این مشاهدات، به جهت عدم امکان مشاهده مستقیم گردابه به شکل سنجاق موی سر و شباهت ویژگی‌های مشاهده شده با ویژگی‌های سایر گردابه‌ها، نمی‌توان به طور دقیق در ارتباط با حضور گردابه به شکل سنجاق موی سر در این شرایط از جریان اظهار نظر نمود.

doi: 10.5829/idosi.ije.2016.29.11b.05